Small-Scale Structure of Strongly Stratified Turbulence

CHRIS R. REHMANN AND JIN HWAN HWANG

Hydrosystems Laboratory, Department of Civil and Environmental Engineering, University of Illinois at Urbana–Champaign, Urbana, Illinois

(Manuscript received 19 December 2003, in final form 30 July 2004)

ABSTRACT

The small-scale structure of turbulence subjected to strong stratification is analyzed with rapid distortion theory to evaluate the performance of formulas for predicting dissipation of turbulent kinetic energy and dissipation of scalar variance. The approach is restricted to weak turbulence in strong stratification, like that in the thermocline or the abyssal ocean. Flows with and without mean shear are considered. For unsheared turbulence, the small scales are axisymmetric about the vertical axis, as others have previously assumed. The calculations here complement and extend previous work because they can be used to compute errors in dissipation estimates, develop simpler formulas, and examine the effects of shear and other parameters. For example, effects of the initial conditions can be significant. For sheared turbulence, the small-scale velocity and buoyancy fields are neither isotropic nor axisymmetric about the vertical axis. Although dissipation formulas based on isotropy work relatively well for unsheared turbulence, some can be incorrect by more than a factor of 3 for sheared turbulence. However, if the mean flow direction can be identified, then a simple and useful dissipation formula can be proposed.

1. Introduction

Vertical mixing is a key component of the global ocean heat and salinity budgets. Direct measurement of vertical mixing is difficult because instrument motions and internal waves occur at the same scales that accomplish the turbulent mixing. Therefore, mixing is frequently estimated by measuring the dissipative scales of the turbulence and inferring eddy diffusivities from simplified budgets of either temperature variance or turbulent kinetic energy (Osborn and Cox 1972; Osborn 1980). Although the indirect methods avoid problems with measuring the large scales of the turbulence, they require more information than can be easily measured. For example, if u_i and T are the fluctuating velocity and temperature, then the dissipation of turbulent kinetic energy and dissipation of temperature variance are defined as

$$\epsilon = \nu\overline{u_{i,j}(u_{i,j} + u_{j,i})} \quad \text{and} \tag{1a}$$

$$\chi_T = 2D\overline{T_{,j}^2}, \tag{1b}$$

where ν is the kinematic viscosity and D is the molecular diffusivity of temperature.[1] Thus, dissipation calculations require nine velocity gradients for ϵ and three temperature gradients for χ_T. While some researchers have measured two of the gradients simultaneously (e.g., Yamazaki et al. 1990), typically only one is available. We use an analytical method to evaluate dissipation formulas and suggest improvements.

To estimate dissipation from a limited number of measured gradients, oceanographers often assume the small scales of the turbulence are isotropic. The reasoning is that if the Reynolds number is large enough, the large, energy-containing scales will be much larger than the small, dissipative scales, and the structure of the small scales will not depend strongly on the forcing (e.g., Tennekes and Lumley 1989, p. 65). In isotropic turbulence, all mean-squared scalar gradients are equal and simple relations between the mean-squared velocity gradients also exist. A mean-squared gradient in the direction of a velocity component is half as large as one in a direction normal to a velocity component; for example,

$$\overline{u_{1,1}^2} = \frac{1}{2}\overline{u_{1,3}^2}. \tag{2}$$

Corresponding author address: C. R. Rehmann, 374 Town Engineering Building, Department of Civil, Construction, and Environmental Engineering, Iowa State University, Ames, IA 50011. E-mail: rehmann@iastate.edu

[1] Standard index notation is used here and throughout the paper. For example, $u_{i,j} = \partial u_i/\partial x_j$, $\overline{T_{,j}^2} = \overline{(\partial T/\partial x_j)^2}$, and repeated indices indicate summation.

The simple structure of isotropic turbulence allows the dissipations to be estimated from one gradient each. The dissipation of turbulent kinetic energy can be estimated with

$$\epsilon = 15\nu\overline{u_{1,1}^2}, \tag{3}$$

and the dissipation of temperature variance can be estimated with

$$\chi_T = 6D\overline{T_{,3}^2}. \tag{4}$$

The use of isotropy is appealing, but several studies suggest that isotropy may not hold for the velocity field in a stratified fluid. Gargett et al. (1984) found that their observations of velocity spectra in a tidal channel could be classified by $\epsilon/\nu N^2$ and they concluded that small-scale isotropy occurs for $\epsilon/\nu N^2 > 200$. Deviations from isotropic behavior occur as $\epsilon/\nu N^2$ decreases. For example, as Van Atta (1991) noted, spectra of $\partial u_3/\partial x_1$ and $\partial u_2/\partial x_1$ measured in the ocean thermocline (from Yamazaki 1990) agree over all but the largest wavenumbers when $\epsilon/\nu N^2 = 361$, as isotropy requires. However, in measurements with $\epsilon/\nu N^2 = 18$ and 64 the spectra of $\partial u_3/\partial x_1$ fall below those of $\partial u_2/\partial x_1$ over a large range of wavenumber. Similar results are observed in laboratory experiments and numerical simulations (Van Atta 1991). In stratified wind tunnel experiments with and without mean shear the ratio $\overline{u_{3,1}^2}/\overline{u_{1,1}^2}$ quickly decreases below 2, the value in isotropic turbulence (Thoroddsen and Van Atta 1992; Piccirillo and Van Atta 1997). Numerical simulations of sheared, stratified, homogeneous turbulence with $50 < \epsilon/\nu N^2 < 650$ show that ϵ estimated with isotropy can be inaccurate by a factor of 2–4 (Itsweire et al. 1993). Smyth and Moum (2000) used direct numerical simulations of turbulence due to Kelvin–Helmholtz instability to conclude that isotropic approximations work well for $\epsilon/\nu N^2 > 100$ but perform worse for smaller values.

Strong stratification and shear can disrupt the isotropy of the scalar field also. Field observations of scalar microstructure in the upper North Atlantic show anisotropy when the Cox number $C = K_T/D$ is less than 10^4 (Sherman and Davis 1995). As with the velocity field, laboratory experiments on unsheared, stratified turbulence show that anisotropy develops soon after the turbulence is generated (Thoroddsen and Van Atta 1992). In fact, Sreenivasan (1991) concluded that isotropy of the small-scale scalar field in a shear flow will occur only for extreme Reynolds numbers. The simulations of Itsweire et al. (1993) suggest that χ_T computed assuming isotropy and using the streamwise gradient would be underestimated by a factor of 4. Smyth and Moum (2000) obtained similar results, though they stated that isotropic approximations of χ_T should be accurate to $O(10\%)$ for $C > 100$.

The results from the studies reviewed above have been used to improve dissipation formulas by adjusting the coefficients in the isotropy relations. Yamazaki and Osborn (1990) used a different approach: They recognized that when stratification is important enough to affect the small scales, it would differentiate the vertical direction from the others. Thus, they derived dissipation formulas assuming that the small scales will be axisymmetric about the vertical. In general, the axisymmetric formulas require four mean-squared velocity gradients, but, using results of previous field experiments, Yamazaki and Osborn (1990) developed formulas for upper and lower bounds on the dissipation that require only two gradients. [Their paper contains an error that was corrected in Yamazaki and Osborn (1993).] Shear due to flow in a horizontal direction breaks axisymmetry around the vertical. Smyth and Moum (2000) found that for their flow dissipation formulas based on axisymmetry around the flow direction perform about as well as the isotropic formulas.

To estimate errors in dissipation formulas in strongly stratified flows, we examine the small-scale structure of the velocity and scalar fields using rapid distortion theory (RDT). As discussed in section 2, because the theory requires the eddy time scales to be large in comparison with the time scale of the mean flow, the results are restricted to weak turbulence in strong stratification such as that found in the thermocline, background areas, and parts of the Equatorial Undercurrent. The theory also complements previous experiments and simulations by allowing a wider parameter range to be explored. For unsheared turbulence (section 3), RDT predicts the small scales to be axisymmetric about the vertical, as Yamazaki and Osborn (1990) assumed. It allows their work to be extended by providing dissipation estimates from a single measured gradient. When shear is added (section 4), axisymmetry no longer holds, but RDT offers guidance for estimating dissipation. The main results and recommendations are summarized in section 5.

2. Rapid distortion theory

Several researchers have used RDT or similar analyses to study homogeneous turbulence in a stratified fluid. For example, Deissler (1962) computed energy spectra for weak turbulence subjected to stratification, and Pearson and Linden (1983) analyzed the final period of decay of stratified turbulence with a linearized theory. Hanazaki and Hunt (1996) found that RDT can explain some of the phenomena, such as upgradient fluxes, observed in unsheared, stratified grid turbulence experiments, while Hunt et al. (1988) used RDT to propose new models of sheared, stratified turbulence.

a. Assumptions

Rapid distortion theory is based on an approximation of the equations for the fluctuating velocities u_i, pressure p, and buoyancy $b = -g\alpha T$, where α is the thermal expansion coefficient. For homogeneous turbulence, in which gradients of averaged turbulence quantities are

zero, the equations for fluctuating quantities in a fluid with a vertical temperature gradient are

$$\frac{\partial u_i}{\partial x_i} = 0, \tag{5a}$$

$$\frac{\partial u_i}{\partial t} + U_j \frac{\partial u_i}{\partial x_j} = -u_j \frac{\partial U_i}{\partial x_j} - \frac{\partial}{\partial x_j}(u_i u_j) - \frac{1}{\rho_0}\frac{\partial p}{\partial x_i} - b\delta_{i3} + \nu \frac{\partial^2 u_i}{\partial x_j^2}, \quad \text{and} \tag{5b}$$

$$\frac{\partial b}{\partial t} + U_j \frac{\partial b}{\partial x_j} = u_3 N^2 - \frac{\partial}{\partial x_j}(b u_j) + D\frac{\partial^2 b}{\partial x_j^2}, \tag{5c}$$

where U_i is the mean velocity, $N = (g\alpha d\overline{T}/dx_3)^{1/2}$ is the buoyancy frequency, and gravity acts in the negative x_3 direction.

The momentum and buoyancy equations, (5b) and (5c), can be linearized under certain conditions. RDT applies when the time scale of the mean flow is small compared to the time scales of the eddies. In this case the mean flow distorts the eddies before they can interact, and thus nonlinear interactions are relatively unimportant (Hunt 1978; Townsend 1980). For a stratified flow in which the mean flow time scale is the gravitational adjustment time N^{-1}, Hanazaki and Hunt (1996) found that RDT applies after one buoyancy period to eddies of size λ and larger if the Froude number is small:

$$\mathrm{Fr}_\lambda = \frac{u_\lambda}{N\lambda} < 1, \tag{6}$$

where u_λ is the velocity associated with eddies of size λ.

For RDT to apply to the dissipative scales, a Froude number based on the velocity and length scales of the small eddies must be small. Model spectra developed by Tennekes and Lumley (1989, their section 8.4) can be used to show that about 90% of the dissipation is obtained by integrating dissipation spectra up to $k(\nu^3/\epsilon)^{1/4} = 1$, or a length scale $\lambda = 2\pi(\nu^3/\epsilon)^{1/4}$. The velocity at scale λ can be estimated as $u_\lambda \approx (\epsilon\lambda)^{1/3}$ (Landau and Lifshitz 1987). Substituting these results into (6) yields

$$\frac{\epsilon}{\nu N^2} < O(10). \tag{7}$$

Reviews by Moum (1997) and Gregg (1998) show that $\epsilon/\nu N^2$ will often be much higher in relatively energetic flows such as mixed layers, tidal channels, and hotspots near topographic features. However, low values of $\epsilon/\nu N^2$ can occur in the thermocline (Gregg 1989; Yamazaki 1990), parts of the Equatorial Undercurrent (Gregg 1998), and "background areas," or areas in which breaking internal waves drive the mixing without effects from topography or mesoscale features (Gregg 1998). In addition to providing dissipation formulas for areas with weak turbulence, RDT also allows uncertainty to be estimated in the extreme case of strong stratification. In particular, if the isotropic formulas perform adequately for the strongly stratified, weak turbulence considered here, they should be adequate for most oceanic situations.

b. Calculations

We treat homogeneous turbulence in a fluid subjected to linear density and velocity profiles, or constant buoyancy frequency N and shear $S = dU_1/dx_3$. If the assumptions in the previous subsection apply, then the nonlinear terms in (5) can be neglected. The solution of the resulting system by Fourier methods is facilitated by transforming to a coordinate system that follows the mean flow (Rogallo 1981):

$$\xi_1 = x_1 - Stx_3, \xi_2 = x_2, \quad \text{and} \quad \xi_3 = x_3. \tag{8}$$

We introduce a Fourier representation of the dependent variables; for example,

$$u_j(\underline{\xi}, t) = \sum_{\underline{\kappa}} \hat{u}_j(\underline{\kappa}, t) e^{-i\kappa_j \xi_j}, \tag{9}$$

where κ_j is the wavenumber in the j direction, $i = \sqrt{-1}$, and the carets denote Fourier amplitudes. Then, when the pressure is eliminated with the continuity equation, the resulting system is

$$\frac{d\hat{u}_1}{dt} = S\left(\frac{2\kappa_1^2}{K^2} - 1\right)\hat{u}_3 + \frac{\kappa_1 K_3}{K^2}\hat{b} - \nu K^2 \hat{u}_1, \tag{10a}$$

$$\frac{d\hat{u}_2}{dt} = 2S\frac{\kappa_1\kappa_2}{K^2}\hat{u}_3 + \frac{\kappa_2 K_3}{K^2}\hat{b} - \nu K^2 \hat{u}_2, \tag{10b}$$

$$\frac{d\hat{u}_3}{dt} = 2S\frac{\kappa_1 K_3}{K^2}\hat{u}_3 + \left(\frac{K_3^2}{K^2} - 1\right)\hat{b} - \nu K^2 \hat{u}_3, \tag{10c}$$

and

$$\frac{d\hat{b}}{dt} = N^2 \hat{u}_3 - DK^2 \hat{b}, \tag{10d}$$

where $\hat{b}$ is the Fourier amplitude of the buoyancy fluctuation and

$$K_3 = \kappa_3 - \kappa_1 St, \tag{11a}$$

$$K^2 = \kappa^2 - 2\kappa_1\kappa_3 St + \kappa_1^2 (St)^2, \quad \text{and} \tag{11b}$$

$$\kappa^2 = \kappa_m \kappa_m. \tag{11c}$$

To complete the solution, one can solve the system (10) and compute the spectra E_{ij} with a discrete Fourier transform of the two-point correlations:

$$E_{ij}(\kappa, t) = \lim_{V\to\infty} \frac{V}{(2\pi)^3} \langle \hat{u}_i \hat{u}_j^\dagger \rangle, \tag{12}$$

where the dagger superscript denotes the complex conjugate and the angle brackets denote an ensemble average. Then, turbulence statistics, such as mean-squared velocity gradients, can be computed by integrating the spectra over wavenumber space:

$$\overline{u_{\alpha,\beta}^2} = \int_{\underline{\kappa}} k_\beta^2 E_{\alpha\alpha}(\underline{\kappa}, t)\, d^3\underline{\kappa}, \tag{13}$$

where Greek indices are not summed.

Analytical expressions for the Fourier amplitudes can be found for the cases with no shear (Hunt et al. 1988; Hanazaki and Hunt 1996), no stratification (e.g., Townsend 1980), and nonzero shear and stratification (Hanazaki and Hunt 2004). One can also derive equations for the spectra and solve them numerically. Because the analytical solutions involve special functions or integrals that must be evaluated numerically, the latter approach is used here. For example, the equation for the cospectrum of vertical velocity and buoyancy is

$$\frac{dE_{b3}}{dt} = 2S\frac{\kappa_1 K_3}{K^2}E_{b3} + \left(\frac{K_3^2}{K^2} - 1\right)E_{bb} + N^2 E_{33} - (\nu + D)K^2 E_{b3}. \tag{14}$$

We consider several initial conditions for the calculations. For most of the calculations we use isotropic spectra:

$$E_{ij}(\underline{\kappa}, 0) = \frac{E(\kappa)}{4\pi\kappa^2}\left(\delta_{ij} - \frac{\kappa_i\kappa_j}{\kappa^2}\right). \tag{15}$$

This spectrum requires that only the energy spectrum function $E(\kappa)$ be specified. For this we use an energy spectrum function similar to that used by Townsend (1980, p. 85):

$$E(\kappa) = \frac{q_0^2}{3\sqrt{2\pi}}\kappa^4\mathcal{L}^5 e^{-(\kappa\mathcal{L})^2/2}, \tag{16}$$

where $\mathcal{L}$ is related to the longitudinal integral scale and $q_0^2/2 = \int_0^\infty E(\kappa)\,d\kappa$ is the initial turbulent kinetic energy.

If the RDT equations are made nondimensional by scaling lengths with $\mathcal{L}$ and time with N^{-1}, molecular viscosity and diffusivity can be parameterized by the Grashof number $\mathrm{Gr} = N\mathcal{L}^2/\nu$ and Schmidt number $\mathrm{Sc} = \nu/D$. The Grashof number, which arises in the ratio of the second and third terms on the right side of Eq. (10c), measures the relative importance of buoyancy and viscous forces. Data in Yamazaki (1990) can be used to find that Gr ranges from 10^2 to 10^3 in the thermocline and fjords. The Schmidt number for heated water is 7, and the Schmidt number for saltwater is 700.

To assess the importance of the initial turbulence structure we also use axisymmetric initial conditions (Maxey 1982):

$$E_{ij}(\underline{\kappa}, 0) = B_1(\kappa)\left(\delta_{ij} - \frac{\kappa_i\kappa_j}{\kappa^2}\right) + B_2(\kappa) \times \left[e_i e_j + \frac{(\kappa_m e_m)^2}{\kappa^2}\delta_{ij} - \frac{\kappa_m e_m(e_i\kappa_j + e_j\kappa_i)}{\kappa^2}\right], \tag{17}$$

where e_i is a unit vector in the direction of the axis of symmetry. In particular, we consider two cases: one in which the axis of symmetry is vertical and one in which the axis of symmetry is normal to both the vertical and mean flow directions; that is, $e_i = \delta_{i3}$ and $e_i = \delta_{i2}$, respectively. In general one must specify both functions $B_1(\kappa)$ and $B_2(\kappa)$, but if the fluid is inviscid or if $\nu = D$, then integrals of these two functions may be specified (Maxey 1982). For the calculation of mean-squared strain rates, we specify

$$\overline{B_n} = \frac{8\pi}{15\gamma_0^2}\int_0^\infty \kappa^4 B_n(\kappa)\,d\kappa, \tag{18}$$

where $n = 1$ or 2 and γ_0^2 is the initial value of $\overline{u_{3,3}^2}$. Using a method similar to Maxey's, one can express $\overline{B_1}$ and $\overline{B_2}$ in terms of the initial value of $\beta_1 = \overline{u_{3,3}^2}/\overline{u_{2,1}^2}$. When the axis of symmetry is vertical,

$$\overline{B_1} = \frac{1}{3}\left(\frac{2}{\beta_1} - 1\right) \quad \text{and} \tag{19a}$$

$$\overline{B_2} = \frac{2}{3}\left(2 - \frac{1}{\beta_1}\right), \tag{19b}$$

and when the axis of symmetry is transverse,

$$\overline{B_1} = 2 - \frac{1}{2\beta_1} \quad \text{and} \tag{20a}$$

$$\overline{B_2} = \frac{1}{\beta_1} - 2. \tag{20b}$$

If the turbulence is isotropic initially $\beta_1 = 1/2$, then $\overline{B_1} = 1$, $\overline{B_2} = 0$, and the spectra in (17) reduce to the isotropic spectra (15).

Initial buoyancy fluctuations can be included relatively easily if the spectrum function of the buoyancy field and the energy spectrum function have the same wavenumber dependence. In this case, only the initial ratio of turbulent potential energy and turbulent kinetic energy needs to be specified (Hanazaki and Hunt 1996). We follow Hunt et al. (1988) and define this ratio in terms of the vertical velocity's contribution to the kinetic energy:

$$\eta_0 = \frac{\overline{b^2}(0)}{\overline{u_3^2}N^2}. \tag{21}$$

With this definition of η_0, the initial spectrum of the buoyancy fluctuations is

$$E_{bb}(\underline{\kappa}, 0) = \frac{E(\kappa)}{4\pi\kappa^2}\left(\frac{2}{3}N^2\eta_0\right). \tag{22}$$

After the initial conditions for the spectra are specified, the equations for either the Fourier components or the spectra can be solved. When there is no mean shear ($S = 0$), viscosity, and diffusion, we obtain analytical expressions for the mean-squared velocity and buoyancy gradients. Otherwise, the spectral equations are solved numerically with a fourth-order Runge–Kutta method with adaptive time stepping. Several tests were done to ensure adequate resolution in wavenumber space since spectra become concentrated in a small area at large times (Rogers 1991).

3. Unsheared, stratified turbulence

In this section we examine the small-scale structure of turbulence in a stratified fluid without mean velocity gradients or shear. For this case the system (10) becomes

$$\frac{d\hat{u}_1}{dt} = \frac{\kappa_1\kappa_3}{\kappa^2}\hat{b} - \nu\kappa^2\hat{u}_1, \tag{23a}$$

$$\frac{d\hat{u}_2}{dt} = \frac{\kappa_2\kappa_3}{\kappa^2}\hat{b} - \nu\kappa^2\hat{u}_2, \tag{23b}$$

$$\frac{d\hat{u}_3}{dt} = \left(\frac{\kappa_3^2}{\kappa^2} - 1\right)\hat{b} - \nu\kappa^2\hat{u}_3, \quad \text{and} \tag{23c}$$

$$\frac{d\hat{b}}{dt} = N^2\hat{u}_3 - D\kappa^2\hat{b}. \tag{23d}$$

Hanazaki and Hunt (1996) have solved this set of equations analytically for the Fourier amplitudes and spectra, and this information can be used to analyze the mean-squared velocity and buoyancy gradients. After considering initially isotropic turbulence with no initial density fluctuations, we consider the effect of nonzero initial density fluctuations and different initial structure.

a. Initially isotropic turbulence

The small-scale structure of the velocity and buoyancy fields is not isotropic, though it is axisymmetric about the vertical as Yamazaki and Osborn (1990) assumed. For an inviscid, nondiffusive fluid ($\nu = D = 0$), the mean-squared gradients for isotropic initial conditions are

$$\overline{u_{1,1}^2} = \overline{u_{2,2}^2} = \frac{2}{15}A\left\{1 - \frac{3}{16}\left(1 - \frac{2}{3}\eta_0\right)\left[1 - \frac{15}{4}I_{3,2}(Nt)\right]\right\}, \tag{24a}$$

$$\overline{u_{1,2}^2} = \overline{u_{2,1}^2} = \frac{4}{15}A\left\{1 - \frac{1}{32}\left(1 - \frac{2}{3}\eta_0\right)\left[1 - \frac{15}{4}I_{3,2}(Nt)\right]\right\}, \tag{24b}$$

$$\overline{u_{1,3}^2} = \overline{u_{2,3}^2} = \frac{4}{15}A\left\{1 - \frac{3}{16}\left(1 - \frac{2}{3}\eta_0\right)\left[1 - \frac{5}{2}I_{1,4}(Nt)\right]\right\}, \tag{24c}$$

$$\overline{u_{3,1}^2} = \overline{u_{3,2}^2} = \frac{2}{15}A\left[\left(1 + \frac{2}{3}\eta_0\right) + \frac{15}{16}\left(1 - \frac{2}{3}\eta_0\right)I_{5,0}(Nt)\right], \tag{24d}$$

$$\overline{u_{3,3}^2} = \frac{1}{15}A\left[\left(1 + \frac{2}{3}\eta_0\right) + \frac{15}{4}\left(1 - \frac{2}{3}\eta_0\right)I_{3,2}(Nt)\right], \tag{24e}$$

$$\overline{b_{,1}^2} = \overline{b_{,2}^2} = \frac{1}{3}AN^2\left[\left(1 + \frac{2}{3}\eta_0\right) - \frac{3}{4}\left(1 - \frac{2}{3}\eta_0\right)I_{3,0}(Nt)\right], \tag{24f}$$

and

$$\overline{b_{,3}^2} = \frac{1}{3}AN^2\left[\left(1 + \frac{2}{3}\eta_0\right) - \frac{3}{2}\left(1 - \frac{2}{3}\eta_0\right)I_{1,2}(Nt)\right], \tag{24g}$$

where

$$A = \int_0^\infty \kappa^2 E(\kappa)\, d\kappa$$

and

$$I_{m,n}(Nt) = \int_0^\pi \sin^m\theta \cos^n\theta \cos(2Nt\sin\theta)\, d\theta, \tag{25}$$

which can be expressed in terms of Struve functions (L. Glasser 1995, personal communication). Time series of these quantities for $\eta_0 = 0$ are normalized by either $\epsilon/\nu = \overline{u_{i,j}^2}$ or $\chi/2D = \overline{b_{,j}^2}$ and plotted against buoyancy time Nt in Figs. 1a and 1b. The axisymmetry about the vertical is not surprising since the isotropic initial conditions are axisymmetric about the vertical (and every other direction) and the structure of the momentum equations in (23a) and (23b) shows that the two horizontal directions are indistinguishable.

For the case of $\eta_0 = 0$ Table 1 summarizes the errors in dissipation incurred by assuming isotropy and computing ε from the average value of a single gradient. Because the mean-squared gradients approach their average values as Nt increases, an asymptotic expansion method can be used to determine the average values. The method of stationary phase (Bleistein and Handelsman 1986, section 6.1) shows that the amplitude of the integrals in (24) decreases as $(Nt)^{-1/2}$ as $Nt \to \infty$. Thus, the average values are obtained simply by ignoring the integrals. Values of ϵ computed with a gradient of a horizontal velocity component are 8%–30% high, while dissipation computed with a gradient of the vertical velocity is 33% low (Fig. 1a). Unlike the velocity field, the density field (Fig. 1b) is isotropic asymptotically. For unsheared, initially isotropic turbulence, es-

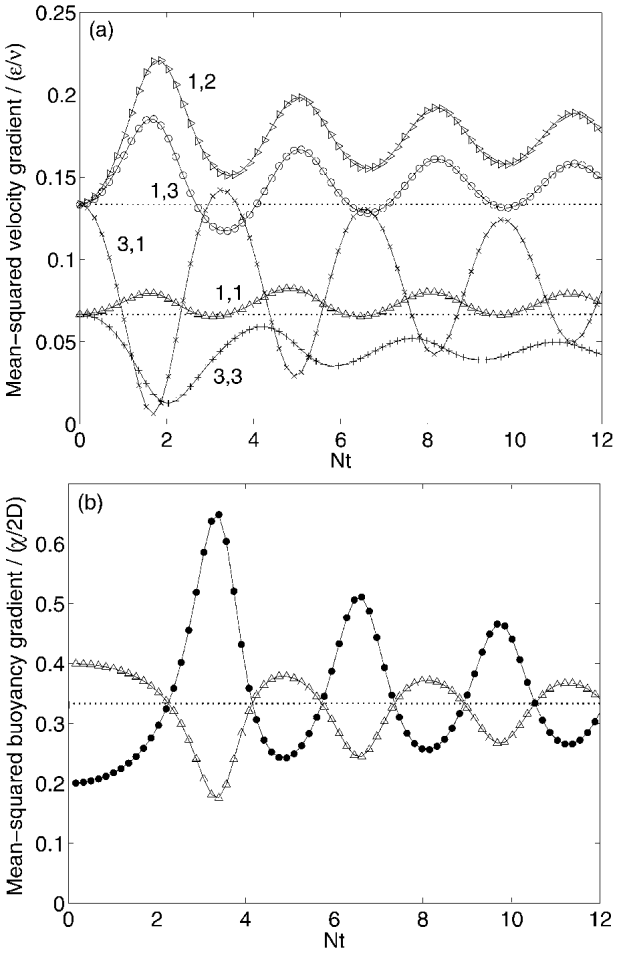

FIG. 1. Mean-squared gradients for inviscid, unsheared, initially isotropic turbulence with no initial buoyancy fluctuations. (a) Velocity gradients normalized by ϵ/ν, Δ: $\overline{u_{1,1}^2} = \overline{u_{2,2}^2}$; $\triangleright$: $\overline{u_{1,2}^2} = \overline{u_{2,1}^2}$; $\circ$: $\overline{u_{1,3}^2} = \overline{u_{2,3}^2}$; $\times$: $\overline{u_{3,1}^2} = \overline{u_{3,2}^2}$; $+$: $\overline{u_{3,3}^2}$. (b) Buoyancy gradients normalized by $\chi/2D$, Δ: $\overline{b_{,1}^2} = \overline{b_{,2}^2}$; $\bullet$: $\overline{b_{,3}^2}$. In both plots the dotted lines indicate the ratios for isotropic turbulence. The isotropic value is not achieved initially in (b) because the buoyancy gradients and χ are initially zero.

timates of χ using the isotropic assumption are quite accurate for both horizontal and vertical gradients.

RDT predicts that viscous effects do not alter the results for the scalar field, but they do affect the velocity field for low Gr (Table 1). An asymptotic analysis similar to that of Hanazaki and Hunt (1996) shows that for large Nt all of the mean-squared buoyancy gradients are equal, regardless of the strength of viscous and diffusive effects. For the velocity field, viscous effects drive the normalized gradients toward isotropic values. For $\mathrm{Gr} = 10^3$ the dissipation errors are close to the values in the inviscid case ($\mathrm{Gr} \to \infty$) and they approach zero as Gr decreases, or viscosity becomes more important. Schmidt number effects are important only at low Gr.

These results can also be compared with those from previous field measurements. For example, the axisymmetric turbulence formulas developed by Yamazaki and Osborn (1990) were motivated by three observations from the oceanic measurements of Osborn and Lueck (1985) and Yamazaki et al. (1990): 1) $\overline{u_{1,3}^2} \approx \overline{u_{2,3}^2}$, 2) $\overline{u_{2,3}^2} \approx \overline{u_{2,1}^2}$, and 3) $\overline{u_{3,1}^2} \approx \overline{u_{2,1}^2}$ when $\epsilon/\nu N^2 > 20$, and $\overline{u_{3,1}^2} < \overline{u_{2,1}^2}$ when $\epsilon/\nu N^2 < 20$. For initially isotropic, unsheared turbulence, calculations from RDT are consistent with these observations. RDT predicts that $\overline{u_{1,3}^2}$ and $\overline{u_{2,3}^2}$ are identically equal, that $\overline{u_{2,3}^2}$ and $\overline{u_{2,1}^2}$ are equal within 20%–25%, and that $\overline{u_{3,1}^2} < \overline{u_{2,1}^2}$. Since RDT for the small scales holds when $\epsilon/\nu N^2$ is small, the last result is consistent with that of Osborn and Lueck (1985) and Yamazaki et al. (1990).

Comparing with results from laboratory experiments and numerical simulations can indicate the usefulness and limitations of the RDT for predicting the small-scale structure. Figure 2a shows values of $\overline{u_{3,1}^2}/\overline{u_{1,1}^2}$ from RDT for two sets of parameters: the stratified wind tunnel measurements of Thoroddsen and Van Atta (1992) and the numerical simulations of Riley et al. (1981). RDT qualitatively predicts the laboratory results for $Nt < 2$ and the simulation results for somewhat larger buoyancy times, although the results agree quantitatively only for $Nt < 1$. The discrepancy can be attributed to the strength of the stratification. Although $\epsilon/\nu N^2$ and the Froude number based on velocity and length scales of the large eddies become small downstream of the grid in the laboratory experiments, they both can be quite large initially. For example, Thoroddsen and Van Atta (1992) give a range of $0.015 < \epsilon/\nu N^2 < 15\,000$. The smaller initial Froude number of 0.3 in the simulations leads to better agreement with the RDT results. RDT does reproduce the observation that the amplitude of oscillation decreases as viscous effects become stronger (i.e., Gr decreases).

Mean-squared buoyancy gradients from RDT can also be compared with previous results. For example, Fig. 2b shows $\overline{b_{,3}^2}/\overline{b_{,1}^2}$ from RDT, laboratory experiments of Thoroddsen and Van Atta (1996), and the direct numerical simulations of Gerz and Schumann (1991). As in the case of the mean-squared velocity gradients, results from RDT and the numerical simulations compare fairly well for about 0.5 of a buoyancy period ($Nt \approx 3$). Although the laboratory result $\overline{b_{,2}^2}/\overline{b_{,1}^2} = 1.17$ (Thoroddsen and Van Atta 1996) is approximately predicted by RDT, which gives $\overline{b_{,1}^2} = \overline{b_{,2}^2}$, values of $\overline{b_{,3}^2}/\overline{b_{,1}^2}$ from RDT and the laboratory experiments do not compare as well. In particular, the initial values from the laboratory experiments differ substantially from those in the other two datasets. Thoroddsen and Van Atta (1996) concluded that the simulations of Gerz and Schumann (1991) were started from an anisotropic state. However, an analysis of the behavior of the buoyancy gradients in (24f) and (24g) as $Nt \to 0$ shows that the ratio is 1/2, as in the direct numerical simulations.

Dissipation formulas that assume isotropy work well in unsheared turbulence (Table 1); they predict dissipation to within ±33%. Nevertheless, the results in

TABLE 1. Summary of the calculations for unsheared, initially isotropic turbulence with no initial buoyancy fluctuations. Errors in assuming isotropy to compute either ϵ or χ are shown; values for finite Gr cases are based on averages from $0 < Nt < 30$. Also shown is the buoyancy time $(Nt)_{\text{avg}}$ at which the average of the mean-squared gradient is within 5% of the asymptotic or mean value in the inviscid case ($\text{Gr} \to \infty$). A percentage error P can be converted to a factor F by $F = (1 + P/100)^{\text{sgn}(P)}$. For example, an error of −33.3% means the dissipation estimate is low by a factor of 1.5.

	Dissipation error (%)					
		$\text{Gr} = 10^3$		$\text{Gr} = 10^2$		
Gradient	$\text{Gr} \to \infty$	Sc = 7	Sc = 700	Sc = 7	Sc = 700	$(Nt)_{\text{avg}}$
$\overline{u_{1,1}^2}$	8.3	7.8	7.7	2.2	1.2	1.9
$\overline{u_{1,2}^2}$	29.2	26.6	26.0	6.4	2.1	0.2
$\overline{u_{1,3}^2}$	8.3	7.9	7.7	2.5	0.7	2.9
$\overline{u_{3,1}^2}$	−33.3	−30.9	−30.3	−8.4	−3.2	1.7
$\overline{u_{3,3}^2}$	−33.3	−29.7	−29.0	−6.3	−0.8	2.2
$\overline{b_{,1}^2}$	0.0	0.0	0.0	0.0	0.0	1.9
$\overline{b_{,3}^2}$	0.0	0.0	0.0	0.0	0.0	3.2

Table 1 can be used to develop improved dissipation formulas that require only one mean-squared gradient. For example, one can compute TKE dissipation with $\epsilon/\nu\overline{u_{3,3}^2} = 15/(1 - 0.333) = 22.5$ or $\epsilon/\nu\overline{u_{1,3}^2} = (15/2)/(1 + 0.083) = 6.9$. Also, the assumptions behind the simplified formulas of Yamazaki and Osborn (1990) can be assessed. As mentioned above, the turbulence is exactly axisymmetric, as Yamazaki and Osborn (1990) assumed. However, to reduce the number of required gradients from four to two, Yamazaki and Osborn (1990) developed semi-isotropic formulas that give upper and lower bounds on the dissipation. Their analysis is based on the behavior of three gradient ratios:

$$\beta_1 = \frac{\overline{u_{3,3}^2}}{\overline{u_{2,1}^2}}, \quad \beta_2 = \frac{\overline{u_{3,1}^2}}{\overline{u_{2,1}^2}}, \quad \text{and} \quad \beta_3 = \frac{\overline{u_{2,3}^2}}{\overline{u_{2,1}^2}}. \tag{26}$$

The semi-isotropic formulas were developed for $\beta_3 = 1$ (Yamazaki et al. 1990; Yamazaki and Osborn 1993), and the lower bound ϵ_L and upper bound ϵ_U correspond to $\beta_1 = 1$ and $\beta_1 = \beta_2/2$, respectively:

$$\epsilon_L = \nu\left(\frac{11}{2}\overline{u_{2,1}^2} + 2\overline{u_{3,1}^2}\right) \quad \text{and} \tag{27a}$$

$$\epsilon_U = \nu\left(\frac{14}{3}\overline{u_{2,1}^2} + \frac{17}{6}\overline{u_{3,1}^2}\right). \tag{27b}$$

In the inviscid, nondiffusive case, RDT predicts $\beta_3 = 1.19$ and gives mean values of β_1 and β_2 of 0.26 and 0.52, respectively. Therefore, RDT suggests that the upper-bound formula of Yamazaki and Osborn (1990) is more appropriate. In fact, the upper-bound (27b) overpredicts ϵ from RDT by only 5%.

One difficulty with using these results in the field is that the evolution time of the turbulence (i.e., Nt) is unknown. In practice, measurements of the mean-squared gradients are averaged over a certain period of time. To assess the averaging time, the cumulative time average of the mean-squared gradients was compared with the mean or asymptotic values. The averaging time was arbitrarily defined as the time beyond which the cumulative time average is within 5% of the limiting value. This value is conservative because the greatest deviation from the mean value occurs just after the turbulence is generated. Averaging times for all gradients are shown in Table 1. These results suggest that estimates of the mean values of the mean-squared gradients can be obtained by averaging for a time between $0.2N^{-1}$ and $3N^{-1}$.

Applying these guidelines to field measurements is complicated. The sampling interval for profilers can be larger than the required averaging time. For example, in the measurements of Toole et al. (1997), the sampling interval of 3 hours exceeded the averaging time of about 18 minutes for measuring $\overline{u_{3,3}^2}$ in fluid with a buoyancy frequency of 1.5×10^{-3} s^{-1}. The guidelines for averaging time can be applied more easily to measurements from a towed vehicle or submarine. In the experiments of Rehmann and Duda (2000) near the seafloor of the New England continental shelf, the buoyancy frequency of 20 cph leads to an averaging time for mean-squared longitudinal conductivity gradients (ignoring effects of shear) of about 54 s. Much longer records were used to compute averages of the dissipation of conductivity variance; the data came from different horizontal positions but similar density levels.

b. *Effects of initial conditions*

The initial conditions can affect the structure. Inspection of (24) shows that initial buoyancy fluctuations, which are parameterized by the initial energy ratio η_0, do not affect the axisymmetry about the vertical and they do not change the result that on average each of the buoyancy gradients contributes equally to χ. However, initial buoyancy fluctuations do change the mean values of the mean-squared velocity gradients and thus

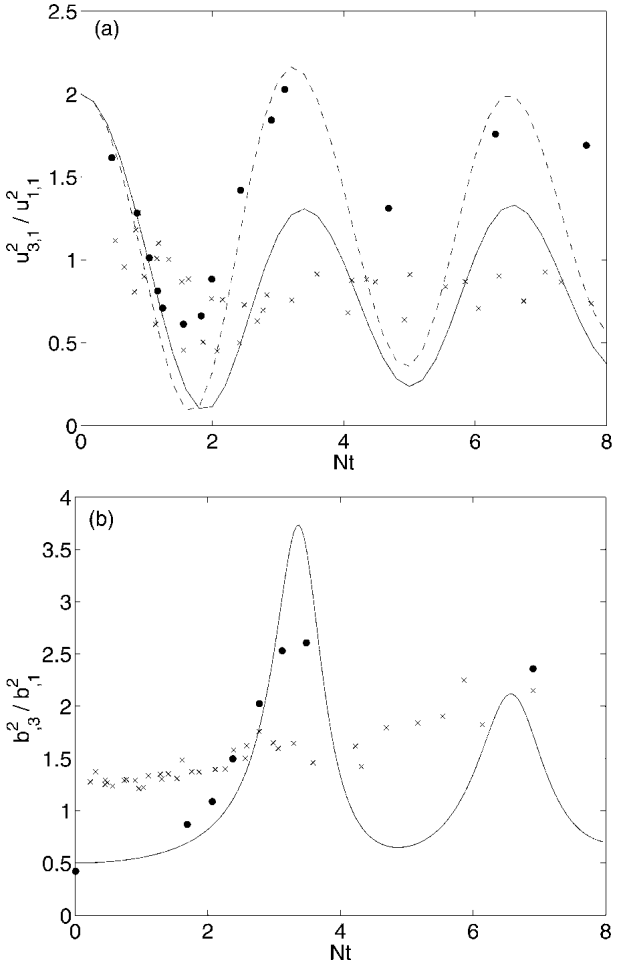

FIG. 2. Comparison with previous results. (a) Mean-squared velocity gradients; dots come from the direct numerical simulation of Riley et al. (1981) with $N = 3.14$ rad s^{-1}, and crosses denote the grid turbulence measurements of Thoroddsen and Van Atta (1992) in a stratified wind tunnel with $N = 3.03$ rad s^{-1}. The lines are computed with RDT; the solid line (Gr = 1.6, Sc = 0.7) corresponds to the experiments of Thoroddsen and Van Atta (1992), while the dashed line (Gr = 83, Sc =1) corresponds to the simulations of Riley et al. (1981). The previous data were taken from Fig. 4 of Thoroddsen and Van Atta (1992). (b) Mean-squared buoyancy gradients; dots come from the direct numerical simulation of Gerz and Schumann (1991), while the crosses denote measurements of Thoroddsen and Van Atta (1996) for $1.25 \leq N \leq 4.03$ rad s^{-1}. The solid line, which is computed with RDT, corresponds to both the experiments and the simulations. The previous data were taken from Fig. 13 of Thoroddsen and Van Atta (1996).

the dissipation estimate errors (Fig. 3). For the range $0 < \eta_0 < 1$, which corresponds to the range studied by Hunt et al. (1988) and Hanazaki and Hunt (1996), an increase in initial buoyancy fluctuations makes the small-scale velocity field more isotropic. In fact, the small scales are exactly isotropic for all time when $\eta_0 = 3/2$, or when by definition [see (21)] the initial turbulent kinetic energy and turbulent potential energy are equal.

Although the performance of ϵ formulas based on isotropy improves as η_0 increases from zero to 3/2, the error in the ϵ estimates increases as η_0 increases further (Fig. 3). The limit $\eta_0 \to \infty$ represents a flow energized by density fluctuations left behind by turbulence that previously decayed (e.g., Gerz and Yamazaki 1993). Equation (24) can be used to show that dissipation estimates based on $\overline{u^2_{1,1}}$, $\overline{u^2_{2,2}}$, $\overline{u^2_{1,3}}$, or $\overline{u^2_{2,3}}$ underestimate ϵ by 25%. Unlike cases with relatively small initial buoyancy fluctuations, estimates of dissipation based on gradients of the vertical velocity overestimate ϵ in buoyancy-generated turbulence. Here all gradients of vertical velocity overpredict ε by 100%. The largest error, however, comes from assuming isotropy and using $\overline{u^2_{1,2}}$ (or $\overline{u^2_{2,1}}$), which underestimates ϵ by 87.5%, or a factor of 8.

The initial structure can also affect the subsequent structure of the turbulence. Specifying the initial structure is somewhat more arbitrary than specifying initial density fluctuations. For $\beta_1 = 1/4$ and $\beta_1 = 1$ we examine inviscid, nondiffusive flows initialized with turbulence axisymmetric about x_3 and flows initialized with turbulence axisymmetric about x_2. As discussed in section 3a, the former value of β_1 is suggested by the study of Yamazaki and Osborn (1990); the latter value is selected simply to examine the dependence on β_1. The case of symmetry about x_3 could represent turbulence that is immediately affected by strong stratification. The case of symmetry about x_2 was chosen to determine whether the stratification forces the flow back to an axisymmetric state.

As in the isotropic case, the velocity gradients approach their mean values as $Nt \to \infty$ when the initial turbulence is axisymmetric about either x_3 or x_2. We

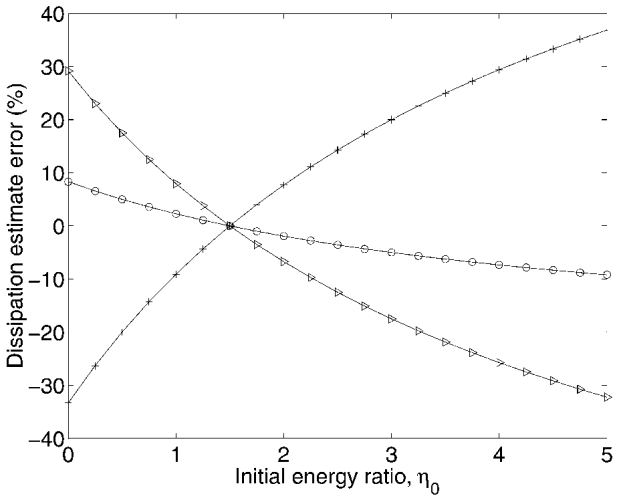

FIG. 3. Errors in dissipation estimates using a single velocity gradient and isotropy as a function of the initial energy ratio η_0. Circles denote the errors for $\overline{u^2_{1,1}} = \overline{u^2_{2,2}}$ and $\overline{u^2_{1,3}} = \overline{u^2_{2,3}}$. Triangles denote the errors for $\overline{u^2_{1,2}} = \overline{u^2_{2,1}}$. Crosses denote the errors for $\overline{u^2_{3,1}} = \overline{u^2_{3,2}}$ and $\overline{u^2_{3,3}}$.

derive the mean values with the method of stationary phase and compute the error incurred by assuming isotropy for cases with $\beta_1 = 1/4$ and $\beta_1 = 1$ (Fig. 4). When the initial turbulence is axisymmetric about x_3, it retains its axisymmetry; for example, the horizontal directions are interchangeable, as in a flow initialized with isotropic turbulence. However, when the initial turbulence is axisymmetric about x_2, axisymmetry about the vertical does not develop. Even though the stratification is strong, effects of the initial structure persist.

The error in dissipation estimates using a single gradient and assuming isotropy depends on the initial value of β_1. In some cases, the error increases and in some it decreases. Estimates based on a gradient of a horizontal velocity component either slightly underestimate ϵ or overpredict it by 5%–70%. As in the isotropic case, the largest errors occur when a gradient of the vertical velocity component is used. For example, when $\beta_1 = 1/4$, which corresponds to the conditions Yamazaki and Osborn (1990) used to develop their upper-bound formula, ϵ can be low by about 50% when the initial turbulence is symmetric about x_3 and about 30%–80% when the initial turbulence is symmetric about x_2.

Errors in estimating χ can also be evaluated. As in the case of initially isotropic turbulence, the isotropic assumption works well for a flow initialized with turbulence symmetric about x_3. That is, on average each of the buoyancy gradients makes up one-third of the scalar variance. For a flow initialized with turbulence symmetric about x_2 the vertical gradient also contributes one third of the scalar variance. However, the amounts from the two horizontal gradients vary with the initial value of β_1. In particular, the method of stationary phase can be used to show that

$$\frac{3\overline{b_{,1}^2}}{\chi/2D} = \frac{3}{2} - \frac{1}{4\beta_1} \quad \text{and} \tag{28a}$$

$$\frac{3\overline{b_{,2}^2}}{\chi/2D} = \frac{1}{2} + \frac{1}{4\beta_1}. \tag{28b}$$

As with the velocity gradients, the error computing χ is larger for $\beta_1 = 1/4$ than for $\beta_1 = 1$; using $\overline{b_{,2}^2}$ overestimates χ by 50% and using $\overline{b_{,1}^2}$ underestimates χ by 50%.

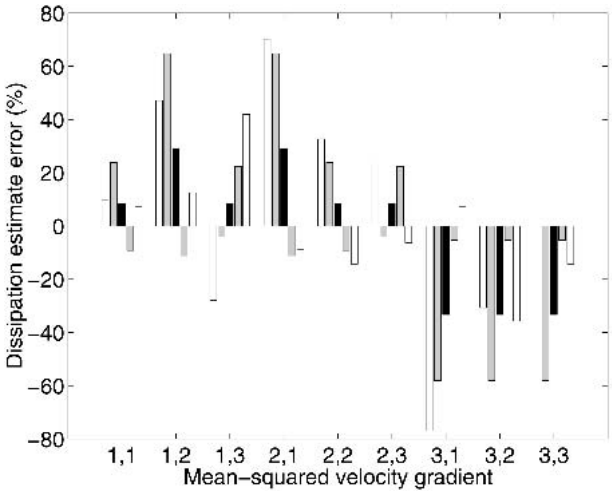

FIG. 4. Errors in dissipation estimates using a single velocity gradient and isotropy for flows with different initial structure. The black bars correspond to isotropic initial conditions ($\beta_1 = 1/2$), and the white and gray bars corresponds to initial conditions with symmetry about the x_2 axis and the x_3 axis, respectively. In each group, the two leftmost bars are for $\beta_1 = 1/4$, while the rightmost two bars are for $\beta_1 = 1$.

4. Sheared, stratified turbulence

In this section we consider the effects of shear on the small-scale structure. Spectral equations like (14) derived from the full (10a)–(10d) for the Fourier amplitudes are solved numerically for different values of the Richardson number $\mathrm{Ri} = (N/S)^2$, and the spectra are integrated to yield the mean-squared gradients. After presenting the results and discussing the main features, we compare with the results of experiments and simulations on sheared, stratified turbulence and discuss the implications of the results for dissipation measurements in the ocean.

The structure of the small-scale velocity and buoyancy fields is not simple. Normalized mean-squared velocity gradients and buoyancy gradients are plotted as functions of dimensionless time St in Figs. 5 and 6 for $\mathrm{Ri} = 0.25$ and $\mathrm{Ri} = 1.0$ and zero viscosity and diffusivity. Only the inviscid, nondiffusive case is plotted because it displays many features also seen in the viscous, diffusive cases. For the parameter range considered the dissipative scales are neither isotropic nor axisymmetric about the vertical, although for large St the velocity field approaches axisymmetry about the vertical for large Ri (Fig. 5b) and the buoyancy field approaches axisymmetry for smaller Ri (Fig. 6a). This lack of simple structure is expected: In cases in which the stratification is strong enough to differentiate the vertical direction from the others the principal axis of the shearing motion will also be important when $S \geq N$, or $\mathrm{Ri} \leq 1$.

Despite the lack of a simple structure, many qualitative features of the evolution of the mean-squared velocity gradients can be observed at all values in the ranges of Richardson, Grashof, and Schmidt numbers. For example, many of the ratios reach approximately constant values within a few eddy turnover times ($\sim S^{-1}$). All gradients of the vertical velocity become small rapidly; except for low Gr and high Ri, each of these gradients contributes less than 5% to the dissipation by about $St = 2$, as in the inviscid case. Also, normalized $\overline{u_{2,2}^2}$ and $\overline{u_{2,3}^2}$ vary relatively little over the times considered even in the viscous, diffusive case. Over the parameter range, the vertical gradient of the buoyancy contributes the most to χ, while $\overline{u_{1,2}^2}$ and $\overline{u_{1,3}^2}$ contribute

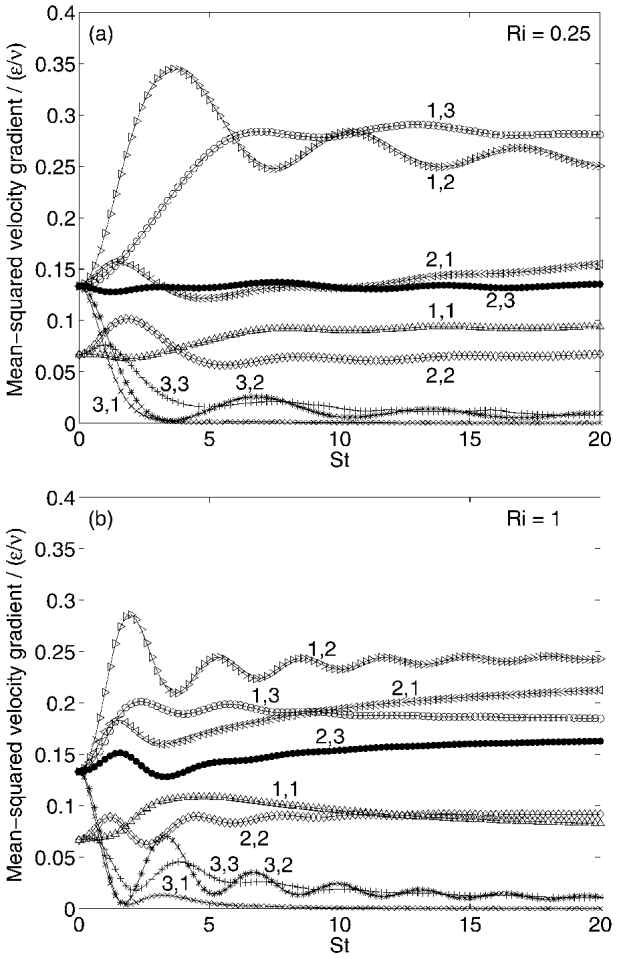

FIG. 5. Mean-squared velocity gradients normalized by ε/ν for inviscid, sheared stratified turbulence with an isotropic initial velocity field, Δ: $\overline{u_{1,1}^2}$; $\triangleright$: $\overline{u_{1,2}^2}$; $\circ$: $\overline{u_{1,3}^2}$; $\triangleleft$: $\overline{u_{2,1}^2}$; $\diamond$: $\overline{u_{2,2}^2}$; $\bullet$: $\overline{u_{2,3}^2}$; $\times$: $\overline{u_{3,1}^2}$; $*$: $\overline{u_{3,2}^2}$; $+$: $\overline{u_{3,3}^2}$; (a) Ri = 0.25, (b) Ri = 1.0.

more than 20% each to the dissipation. A vertical gradient of the x_1 component of mean velocity would be expected to rotate large eddies to be aligned with the x_1 direction and therefore increase the gradients of u_1 in the two normal directions. For the weak turbulence considered here, the shear appears to affect the small eddies too.

Table 2 shows the errors in dissipation estimates that use isotropy as averages from $0 < St < 20$. Isotropic formulas using $\overline{u_{1,2}^2}$ and $\overline{u_{1,3}^2}$ overestimate ϵ, while formulas using gradients of the vertical velocity underestimate ϵ substantially. Isotropic formulas using the vertical buoyancy gradient overestimate χ, while formulas using horizontal buoyancy gradient either underestimate or slightly overestimate χ. The results in Table 2 suggest using the isotropic formula

$$\epsilon = \frac{15}{2}\,\nu\overline{u_{2,3}^2} \tag{29}$$

to estimate the TKE dissipation because it incurs less that 15% error for the parameter range used. Furthermore, because $\overline{u_{2,3}^2}$ varies very little with time (Fig. 5), fewer data would be needed to obtain a converged averaged. As in the case without shear, the results in Table 2 can be used to develop dissipation formulas using any of the gradients; however, $\overline{u_{2,3}^2}$ varies least over the range of Ri and Gr.

The results can also be compared with results from other studies of sheared, stratified turbulence. As in the case of unsheared turbulence, results from RDT are consistent with the field observations of Yamazaki et al. (1990). For $0.25 < \mathrm{Ri} < 1$ and high Gr, $\overline{u_{2,1}^2}$ and $\overline{u_{2,3}^2}$ are comparable, as they are when $S = 0$. Shear makes $\overline{u_{3,1}^2}$ much less than $\overline{u_{2,1}^2}$, or $\beta_2 \ll 1$; such values occur for $\epsilon/\nu N^2 < 10$ (Yamazaki and Osborn 1990). One difference from the unsheared case is that $\overline{u_{1,3}^2}$ exceeds $\overline{u_{2,3}^2}$. Also, RDT produces much lower values of $\overline{u_{3,1}^2}$ than found in laboratory experiments. For example, in the unstratified wind tunnel experiments of Tavoularis and Corrsin (1981) $\overline{u_{3,1}^2}/\overline{u_{1,1}^2}$ was approximately 1.5. When

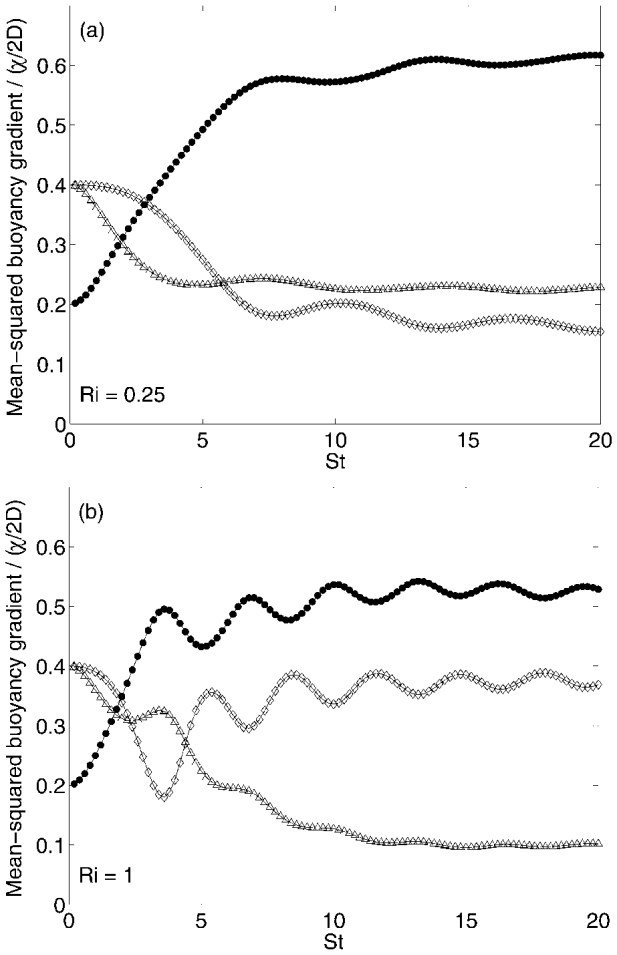

FIG. 6. Mean-squared buoyancy gradients normalized by $\chi/2D$ for inviscid, sheared stratified turbulence with an isotropic initial velocity field, Δ: $\overline{b_{,1}^2}$; $\diamond$: $\overline{b_{,2}^2}$; $\bullet$: $\overline{b_{,3}^2}$; (a) Ri = 0.25, (b) Ri = 1.0.

TABLE 2. Summary of the calculations for sheared, initially isotropic turbulence with no initial buoyancy fluctuations. Errors in assuming isotropy to compute either ϵ or χ are shown. Values are based on averages from $0 < St < 20$.

	Dissipation error (%)					
	Ri = 0.25			Ri = 1		
Gradient	Gr $\to \infty$	Gr = 10^3	Gr = 10^2	Gr $\to \infty$	Gr = 10^3	Gr = 10^2
$\overline{u_{1,1}^2}$	29	−13	−50	38	−17	−54
$\overline{u_{1,2}^2}$	99	121	105	77	120	86
$\overline{u_{1,3}^2}$	94	151	203	40	100	139
$\overline{u_{2,1}^2}$	4	−48	−72	42	−43	−71
$\overline{u_{2,2}^2}$	2	−17	−36	31	12	−9
$\overline{u_{2,3}^2}$	0	−4	−5	14	9	13
$\overline{u_{3,1}^2}$	−93	−93	−93	−94	−94	−93
$\overline{u_{3,2}^2}$	−85	−82	−76	−81	−69	−52
$\overline{u_{3,3}^2}$	−68	−59	−38	−65	−40	21
$\overline{b_{,1}^2}$	−27	−35	−55	−48	−52	−63
$\overline{b_{,2}^2}$	−32	−32	−38	4	0	−10
$\overline{b_{,3}^2}$	58	67	93	44	52	74

the stratification is stronger, however, Piccirillo and Van Atta (1997) found that $\overline{u_{3,1}^2}/\overline{u_{1,1}^2}$ fell below the isotropic value of 2 when $\epsilon/\nu N^2 < 2000$ and reached values between 0.1 and 0.6 for $\epsilon/\nu N^2 < 40$. The results from RDT (Fig. 5) indicate an even stronger effect of the stratification: when $St > 5$, $\overline{u_{3,1}^2}/\overline{u_{1,1}^2}$ is very close to zero.

The small-scale velocity field predicted by RDT shares many features with those from direct numerical simulations of sheared, stratified, homogenous turbulence (Itsweire et al. 1993) and turbulence due to Kelvin–Helmholtz instability (Smyth and Moum 2000). Like the simulations of Itsweire et al. (1993) and cases with low $\epsilon/\nu N^2$ from Smyth and Moum (2000), RDT shows that 1) streamwise gradients are reduced below the isotropic values when Gr is finite, 2) $\overline{u_{1,3}^2}$, $\overline{u_{2,3}^2}$, and $\overline{u_{1,2}^2}$ are the main contributors to the dissipation, and 3) gradients of the vertical velocity are small. For the specific case of Ri = 0.21, Gr = 71, and Sc = 2, RDT overpredicts $\overline{u_{1,2}^2}$ and underpredicts $\overline{u_{2,2}^2}$ and horizontal gradients of vertical velocity found by Itsweire et al. (1993; Fig. 7). However, both RDT and the simulations of Itsweire et al. (1993) show the same trends of the gradients compared to the isotropic values.

The small-scale buoyancy field from RDT is also similar to that in the numerical simulations. RDT predicts that $\overline{b_{,3}^2}$ exceeds the isotropic value, $\overline{b_{,1}^2}$ falls well below the isotropic value, and $\overline{b_{,2}^2}$ is either below or near the isotropic value (Fig. 6 and Table 2). Although the scalar field tends to become isotropic at Cox numbers above 100 in the simulations of Smyth and Moum (2000), the predictions for lower Cox numbers agree qualitatively with the RDT results. For homogenous turbulence with $0.075 < \text{Ri} < 1$, Itsweire et al. (1993) found that estimates of χ based on the vertical buoyancy gradient were up to a factor of 2 high, while estimates based on the streamwise buoyancy gradient were up to a factor of 4 low. The percentages in Table 2 give similar results: RDT predicts that formulas using $\overline{b_{,1}^2}$ overestimate by a factor of 2, and formulas using $\overline{b_{,3}^2}$ underestimate by a factor of about 3.

The results above can be used to evaluate the performance of other formulas for computing the dissipation of turbulent kinetic energy in sheared, stratified turbulence. Table 3 lists errors incurred by using isotropic formulas using two gradients (Yamazaki et al. 1990; Itsweire et al. 1993), the semi-isotropic upper-bound formula for axisymmetric turbulence (Yamazaki and Osborn 1990; Yamazaki and Osborn 1993), a for-

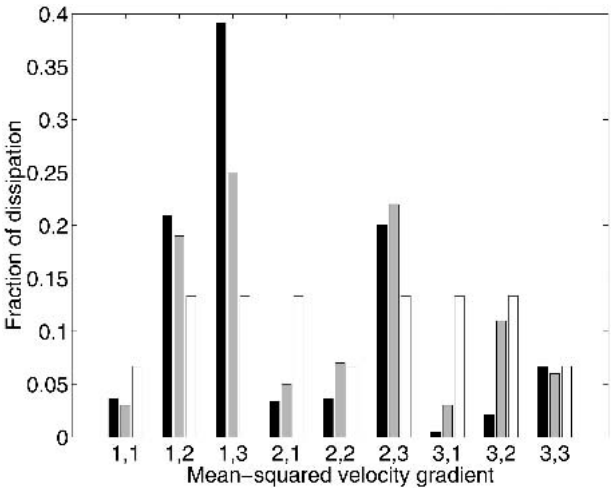

FIG. 7. Contributions of the mean-squared velocity gradients to the dissipation for Ri = 0.21. The black bar in each group comes from RDT with Gr = 71 and Sc = 2, the gray bar comes from the direct numerical simulations of Itsweire et al. (1993), and the white bar is for isotropic turbulence. The data were averaged from $St = 2$ to $St = 8$, as in Itsweire et al. (1993).

TABLE 3. Evaluation of other formulas to compute the dissipation of turbulent kinetic energy.

Formula	Dissipation error (%)					
	Ri $\to \infty$		Ri = 0.25		Ri = 1	
	Gr = 10^3	10^2	10^3	10^2	10^3	10^2
Tow along current direction $\epsilon/\nu = \frac{15}{4}(\overline{u_{2,1}^2} + \overline{u_{3,1}^2})$	−2	−1	−71	−83	−68	−82
Tow across current direction $\epsilon/\nu = \frac{15}{4}(\overline{u_{2,1}^2} + \overline{u_{3,2}^2})$	−2	−1	20	14	25	17
Vertical profile $\epsilon/\nu = \frac{15}{4}(\overline{u_{1,3}^2} + \overline{u_{2,3}^2})$	8	2	73	99	54	76
Yamazaki and Osborn (1993) upper bound $\epsilon/\nu = \frac{14}{3}\left(\overline{u_{2,1}^2} + \frac{17}{6}\overline{u_{3,1}^2}\right)$	5	1	−65	−80	−62	−80
Axisymmetric about x_1 $\epsilon/\nu = -\overline{u_{1,1}^2} + 2\overline{u_{1,2}^2} + 2\overline{u_{2,1}^2} + 8\overline{u_{2,2}^2}$	−2	0	−11	−8	0	19
Equation (29) $\epsilon/\nu = \frac{15}{2}\overline{u_{2,3}^2}$	8	2	−4	−5	9	13

mula assuming axisymmetry about x_1, which Smyth and Moum (2000) tested, and (29). All formulas predict ε within ±25% in unsheared turbulence. For finite Ri both the upper-bound formula of Yamazaki and Osborn (1990) and Yamazaki and Osborn (1993) and the formula based on measurements from towing along the direction of the current substantially underestimate the dissipation, while the large contribution of $\overline{u_{1,3}^2}$ causes the formula that uses a vertical profile to overestimate ϵ. However, towing across the current direction leads to a good estimate. Results from the numerical simulations of Itsweire et al. (1993) and Smyth and Moum (2000) support some of the observations from RDT.

The most consistently accurate formulas are the formula that assumes axisymmetry about x_1 and (29). Both estimate ϵ within ±20%, and both predict the dissipation exactly in isotropic turbulence. Because both dissipation estimates vary little in time (e.g., Fig. 5), relatively short data records would be required to obtain a converged average. One major advantage of (29) is that is requires only one gradient—one that vertically profiling instruments usually measure. In contrast, the formula assuming axisymmetry requires four, or two to three more than are usually measured.

Both formulas (and the others in Table 3) suffer from an additional source of uncertainty that is not present in unsheared turbulence: Unless the x_1 and x_2 directions can be distinguished, results computed with formulas that use any gradients other than $\overline{u_{3,3}^2}$ will be uncertain. For example, if x_1 and x_2 are mistaken for one another—or if u_1 instead of u_2 is measured—the dissipation computed with (29), mistakenly using $\overline{u_{1,3}^2}$ instead of $\overline{u_{2,3}^2}$, can be high by a factor of 2–3. Measuring finescale velocity profiles would help to identify the x_1 and x_2 directions. Also, under the conditions of the RDT (i.e., low $\epsilon/\nu N^2$), $\overline{u_{1,3}^2}$ exceeds $\overline{u_{2,3}^2}$ for Ri ≤ 1.

5. Summary

Because estimates of vertical mixing in the ocean computed from indirect, dissipation-based methods rely on assumptions of a simple small-scale structure, we analyzed the structure theoretically to quantify the effects of anisotropy at the small scales. Assuming that the stratification is very strong, we computed mean-squared velocity and buoyancy gradients with rapid distortion theory (RDT). In this approach, nonlinear, eddy–eddy interactions are neglected because the time scale of the mean flow (e.g., N^{-1}) is assumed to be small compared to the eddy turnover time. Although this assumption restricts the results to flows with small $\epsilon/\nu N^2$, many of the RDT predictions are consistent with results from field, laboratory, and numerical studies. Still, the main use of our work is to evaluate the performance of dissipation formulas in very strongly stratified flows. If the isotropy assumption is adequate in the extreme cases studied here, it should be adequate in typical oceanic cases.

Existing dissipation formulas work well in unsheared, stratified turbulence. Unsheared turbulence that is initially isotropic remains axisymmetric about the vertical direction, as Yamazaki and Osborn (1990) assumed in developing their dissipation formulas. All formulas tested predicted ϵ within ±33%, and the performance improved as viscous effects became stronger. Unlike the velocity field, the density field is isotropic on average; when there is no shear, estimates of χ using the

isotropic assumption are quite accurate for both horizontal and vertical gradients. Effects of the initial conditions can be significant: Assuming isotropy in flows energized by buoyancy fluctuations from previous turbulent events can lead to large errors in ϵ. Also, in cases with no initial symmetry about the vertical, no symmetry develops, and, in the isotropic case, the largest errors occur when a gradient of the vertical velocity component is used.

Shear disrupts the axisymmetry of stratified turbulence and leads to larger errors in some of the dissipation formulas. Gradients of the vertical velocity become small quickly and contribute little to ϵ, while shears of the longitudinal velocity (i.e., $\overline{u_{1,2}^2}$ and $\overline{u_{1,3}^2}$) contribute the most to the dissipation. The small-scale buoyancy field is also anisotropic; a formula for χ based on the vertical buoyancy gradient is a factor of about 2 (i.e., 93%) high, while estimates of χ using $\overline{b_{,1}^2}$ would be low by up to a factor of about 3 (i.e., −63%). The performance of other formulas for ε varies (Table 3); for example, a formula based on vertical profiles overestimates ϵ, while a formula based on tows along the current direction greatly underestimates ϵ. If the direction of the mean flow can be identified, then the isotropic formula

$$\epsilon = \frac{15}{2}\,\nu\overline{u_{2,3}^2}$$

works quite well. This formula has the advantages that it uses a single measured gradient, predicts ε to within 8% for unsheared turbulence as well, and works well for both weak turbulence in strong stratification and more energetic turbulence in which the small scales can be expected to be isotropic. Also, since $\overline{u_{2,3}^2}$ varies little with time, uncertainty introduced by not knowing when the turbulence was generated will be small.

Acknowledgments. We acknowledge the support of the National Science Foundation under Grant 01-17782. Any opinions, findings, and conclusions or recommendations expressed in this material are those of the authors and do not necessarily reflect the views of the National Science Foundation.

REFERENCES

Bleistein, N., and R. A. Handelsman, 1986: *Asymptotic Expansions of Integrals.* Dover, 425 pp.

Deissler, R. G., 1962: Turbulence in the presence of a vertical body force and temperature gradient. *J. Geophys. Res.,* **67,** 3049–3062.

Gargett, A. E., T. R. Osborn, and P. W. Nasymyth, 1984: Local isotropy and the decay of turbulence in a stratified fluid. *J. Fluid Mech.,* **144,** 231–280.

Gerz, T., and U. Schumann, 1991: Direct simulation of homogenous turbulence and gravity waves in sheared and unsheared stratified flows. *Turbulent Shear Flows,* W. C. Reynolds, Ed., Springer, 27–45.

——, and H. Yamazaki, 1993: Direct numerical simulation of buoyancy-driven turbulence in stably stratified fluid. *J. Fluid Mech.,* **249,** 415–440.

Gregg, M. C., 1989: Scaling turbulent dissipation in the thermocline. *J. Geophys. Res.,* **94,** 9686–9698.

——, 1998: Estimation and geography of diapycnal mixing in the ocean. *Physical Processes in Lakes and Oceans,* J. Imberger, Ed., Amer. Geophys. Union, 305–338.

Hanazaki, H., and J. C. R. Hunt, 1996: Linear processes in unsteady stably stratified turbulence. *J. Fluid Mech.,* **318,** 303–337.

——, and ——, 2004: Structure of unsteady stably stratified turbulence with mean shear. *J. Fluid Mech.,* **507**, 1–42.

Hunt, J. C. R., 1978: A review of the theory of rapidly distorted turbulent flows and its applications. *Fluid Dyn. Trans.,* **9,** 121–150.

——, D. D. Stretch, and R. E. Britter, 1988: Length scales in stably stratified turbulent flows and their use in turbulence models. *Stably Stratified Flow and Dense Gas Dispersion,* J. S. Puttock, Ed., Clarendon, 285–321.

Itsweire, E. C., J. R. Koseff, D. A. Briggs, and J. H. Ferziger, 1993: Turbulence in stratified shear flows: Implications for interpreting shear-induced mixing in the ocean. *J. Phys. Oceanogr.,* **23,** 1508–1522.

Landau, L. D., and E. M. Lifshitz, 1987: *Fluid Mechanics.* Pergamon, 539 pp.

Maxey, M. R., 1982: Distortion of turbulence in flows with parallel streamlines. *J. Fluid Mech.,* **124,** 261–282.

Moum, J. N., 1997: Quantifying vertical fluxes from turbulence in the ocean. *Oceanography,* **10,** 111–115.

Osborn, T. R., 1980: Estimates of the local rate of vertical diffusion from dissipation measurements. *J. Phys. Oceanogr.,* **10,** 83–89.

——, and C. S. Cox, 1972: Oceanic finestrucutre. *Geophys. Fluid Dyn.,* **3,** 321–345.

——, and R. G. Lueck, 1985: Turbulence measurements with a submarine. *J. Phys. Oceanogr.,* **15,** 1502–1520.

Pearson, H. J., and P. F. Linden, 1983: The final stage of decay of turbulence in stably stratified fluid. *J. Fluid Mech.,* **134,** 195–203.

Piccirillo, P. S., and C. W. Van Atta, 1997: The evolution of a uniformly sheared thermally stratified turbulent flow. *J. Fluid Mech.,* **334,** 61–86.

Rehmann, C. R., and T. F. Duda, 2000: Diapycnal diffusivity inferred from scalar microstructure measurements near the New England shelf/slope front. *J. Phys. Oceanogr.,* **30,** 1354–1371.

Riley, J. J., R. W. Metcalfe, and M. A. Weissman, 1981: Direct numerical simulations of homogeneous turbulence in density stratified fluids. *Nonlinear Properties of Internal Waves,* B. J. West, Ed., Vol. 76, AIP Conf. Proc., 79–112.

Rogallo, R. S., 1981: Numerical experiments in homogenous turbulence. NASA Tech. Memo. 81315, NASA/Ames Research Center, 53 pp.

Rogers, M. M., 1991: The structure of a passive scalar field with a uniform mean gradient in rapidly sheared homogenous turbulent flow. *Phys. Fluids A,* **3,** 144–154.

Sherman, J. T., and R. E. Davis, 1995: Observations of temperature microstructure in NATRE. *J. Phys. Oceanogr.,* **25,** 1913–1929.

Smyth, W. D., and J. N. Moum, 2000: Anisotropy of turbulence in stably stratified mixing layers. *Phys. Fluids,* **12,** 1343–1362.

Sreenivasan, K. R., 1991: On local isotropy of passive scalars in turbulent shear flows. *Proc. Roy. Soc. London,* **434A,** 165–182.

Tavoularis, S., and S. Corrsin, 1981: Experiments in a nearly homogenous shear flow with uniform mean temperature gradient. Part 2: The fine structure. *J. Fluid Mech.,* **104,** 349–367.

Tennekes, H., and J. L. Lumley, 1989: *A First Course in Turbulence.* The MIT Press, 300 pp.

Thoroddsen, S. T., and C. W. Van Atta, 1992: The influence of

table stratification on small-scale anisotropy and dissipation in turbulence. *J. Geophys. Res.,* **97,** 3647–3658.
——, and ——, 1996: Experiments on density-gradient anisotropies and scalar dissipation of turbulence in a stably stratified fluid. *J. Fluid Mech.,* **322,** 383–409.
Toole, J. M., R. W. Schmitt, K. L. Polzin, and E. Kunze, 1997: Near-boundary mixing above the flanks of a midlatitude seamount. *J. Geophys. Res.,* **102,** 947–959.
Townsend, A. A., 1980: *The Structure of Turbulent Shear Flow*. Cambridge University Press, 429 pp.
Van Atta, C., 1991: Local isotropy of the smallest scales of turbulent scalar and velocity fields. *Proc. Roy. Soc. London,* **434A,** 139–147.
Yamazaki, H., 1990: Stratified turbulence near a critical dissipation rate. *J. Phys. Oceanogr.,* **20,** 1583–1598.
——, and T. Osborn, 1990: Dissipation estimates for stratified turbulence. *J. Geophys. Res.,* **95,** 9739–9744.
——, and ——, 1993: Correction to "Dissipation estimates for stratified turbulence." *J. Geophys. Res.,* **98,** 12 605.
——, R. G. Lueck, and T. Osborn, 1990: A comparison of turbulence data from a submarine and a vertical profiler. *J. Phys. Oceanogr.,* **20,** 1778–1786.